Enhanced Bioelectrocatalysis Using Au-Nanoparticle/Polyaniline Hybrid Systems in Thin Films and Microstructured Rods Assembled on Electrodes

ARTICLE *in* CHEMISTRY OF MATERIALS · SEPTEMBER 2005

Impact Factor: 8.35 · DOI: 10.1021/cm050193v

4 AUTHORS, INCLUDING:

Eran Granot
Hebrew University of Jerusalem
11 PUBLICATIONS **531** CITATIONS

SEE PROFILE

Enhanced Bioelectrocatalysis Using Au-Nanoparticle/Polyaniline Hybrid Systems in Thin Films and Microstructured Rods Assembled on Electrodes

Eran Granot, Eugenii Katz, Bernhard Basnar, and Itamar Willner*

Institute of Chemistry and the Center for Nanotechnology, The Hebrew University of Jerusalem, Jerusalem 91904, Israel

Received January 27, 2005. Revised Manuscript Received June 7, 2005

Composite materials consisting of polyaniline/poly(4-styrene-sulfonate) (PAn/PSS) or polyaniline/Au nanoparticles capped with 2-mercaptoethane sulfonic acid (PAn/Au-NPs) are prepared in the form of thin films (thickness ca. 90 nm) on Au electrodes or in the form of microrods linked to a Au surface. The composite materials in the microrod structures are electrochemically prepared in porous alumina membranes coated with a Au film, followed by the dissolution of the membrane. Chronoamperometric experiments reveal that the charge transport in the PAn/Au-NPs system is ca. 25-fold enhanced as compared to the analogous PAn/PSS system. The different polyaniline composite assemblies were used as catalysts for the electrochemical oxidation of ascorbic acid and as electron-transfer mediators for the bioelectrocatalytic activation of glucose oxidase (GOx) toward the oxidation of glucose. The PAn/Au-NPs system in the microrod structure reveals superior function as the catalyst for the electrochemical oxidation of ascorbic acid and in the bioelectrocatalytic activation of GOx because of the high surface area of the assembly and the enhanced charge-transport properties of the composite material.

Introduction

Hybrid systems consisting of metal or semiconductor nanoparticles and organic compounds became an interesting research topic in recent years.[1] The integration of metal (e.g., Au, Pt, Pd, or Cu) or semiconductor (CdS, CdSe, CdTe, or TiO_2) nanoparticles into polymer matrixes attracts substantial research efforts directed to the development of hybrid materials of new catalytic,[2] electronic,[3] and optoelectronic functionalities.[4] Particularly, the incorporation of metallic or semiconductor nanoparticles in conductive redox polymers, such as polypyrrole[2c,4a] and polyaniline,[2a,3a,4c] is of interest because of strong electronic interactions between the nanoparticles and the polymer matrixes. It has been shown that the electrocatalytic properties of nanoparticles are enhanced by the conductive environment provided by the polymeric matrixes,[2] while the conductivity of the hybrid systems is improved in the presence of metal nanoparticles embedded into the polymers.[3a] Also, aggregated metal nanoparticles included in nonconductive polymers can convert the polymeric matrix into an electrically conductive system. For example, aggregated Cu nanoparticles electrochemically generated in a poly(acrylic acid) thin film associated with an electrode surface resulted in a matrix with conductive properties. The electrochemical dissolution of the Cu nanoclusters in the film resulted in the formation of a nonconductive polymer preserving in its volume Cu^{2+} ions, thus allowing the reversible switching between the conductive and nonconductive states of the hybrid system.[5] The electroswitchable conductivity of the Cu-nanoparticles/poly(acrylic acid)-hybrid system was applied to control the bioelectrocatalytic properties of an enzyme linked to the hybrid system and to design an electrically switchable biofuel cell.[6] Also, electrogenerated Cu nanoclusters in a CdS nanoparticle/poly(acrylic acid) composite system led to the development of an electroswitchable photoelectrochemical system.[7]

Polyaniline (PAn)[8] is a key material in the family of conductive polymers,[9] and numerous studies have addressed its electrochemical[10] and conductivity[11] functions as well as

* Author to whom correspondence should be addressed. Tel: 972-2-658-5272; fax: 972-2-652-7715; e-mail: willnea@vms.huji.ac.il.

(1) Shipway, A. N.; Katz, E.; Willner, I. *ChemPhysChem* **2000**, *1*, 18−52.

(2) (a) Mascaro, L. H.; Gonçalves, D.; Bulhões, L. O. S. *Thin Solid Films* **2004**, *461*, 243−249. (b) O'Mullane, A. P.; Dale, S. E.; Macpherson, J. V.; Unwin, P. R. *Chem. Commun.* **2004**, 1606−1607. (c) Hepel, M. *J. Electrochem. Soc.* **1998**, *145*, 124−134.

(3) (a) Tian, S.; Liu, J.; Zhu, T.; Knoll, W. *Chem. Mater.* **2004**, *16*, 4103−4108. (b) Kulesza, P. J.; Chojak, M.; Karnicka, K.; Miecznikowski, K.; Palys, B.; Lewera, A. *Chem. Mater.* **2004**, *16*, 4128−4134. (c) Sheeney-Haj-Ichia, L.; Sharabi, G.; Willner, I. *Adv. Funct. Mater.* **2002**, *12*, 27−32.

(4) (a) Gaponik, N. P.; Talapin, D. V.; Rogach, A. L.; Eychmüller, A. *J. Mater. Chem.* **2000**, *10*, 2163−2166. (b) Khanna, P. K.; Lonkar, S. P.; Subbarao, V. V. V. S.; Jun, K.-W. *Mater. Chem. Phys.* **2004**, *87*, 49−52. (c) Zhang, L.; Wan, M. *J. Phys. Chem.* **2003**, *107*, 6748−6753. (d) Granot, E.; Patolsky, F.; Willner, *J. Phys. Chem. B* **2004**, *108*, 5875−5881. (e) Pardo-Yissar, V.; Bourenko, T.; Wasserman, J.; Willner, I. *Adv. Mater.* **2002**, *14*, 670−673.

(5) Chegel, V. I.; Raitman, O. A.; Lioubashevski, O.; Shirshov, Y.; Katz, E.; Willner, I. *Adv. Mater.* **2002**, *14*, 1549−1553.

(6) Katz, E.; Willner, I. *J. Am. Chem. Soc.* **2003**, *125*, 6803−6813.

(7) Sheeney-Haj-Ichia, L.; Cheglakov, Z.; Willner, I. *J. Phys. Chem. B* **2004**, *108*, 11−15.

(8) (a) Huang, W.-S.; Humphrey, B. D.; MacDiarmid, A. G. *J. Chem. Soc., Faraday Trans. 1* **1986**, *82*, 2385−2400. (b) Negi, Y. S.; Adhyapak, P. V. *J. Macromol. Sci., Part C* **2002**, *42*, 35−53.

(9) (a) *Handbook of Conducting Polymers*, 2nd ed.; Skotheim, T. A., Elsenbaumer, R. L., Reynolds, J. R., Eds.; Marcel Dekker: New York, 1997. (b) Jagur-Grodzinski J. *Polym. Adv. Technol.* **2002**, *13*, 615−625.

10.1021/cm050193v CCC: $30.25
Published on Web 08/06/2005

its photoelectrochemical properties.[12] Numerous electronic and optoelectronic applications of polyaniline were reported including PAn matrixes for sensing[13] and the electrochemically induced mechanical activation of the movement of microobjects.[14] Specifically, polyaniline was employed as a redox polymer for the electrochemical activation of redox enzymes and for the development of electrochemical and optical biosensors. The amperometric responses of the polymer/enzyme electrodes[15] and the change in the optical properties of the polymer upon the redox transformation were used as electrochemical or optical (surface plasmon resonance)[16] readout signals for the biosensing processes, respectively.

Polyaniline, by itself, reveals redox functions only in acid media, pH < 3,[17] a feature that limits its broad use, specifically in combination with biomaterials. It was, however, reported that the doping of PAn with anionic species or the formation of composite polymer blends between PAn and negatively charged polymers such as polystyrene sulfonate or poly(acrylic acid) switches the redox activity of PAn to neutral pH values in aqueous media.[18]

Here, we wish to report on the electrochemical characterization of a new composite material consisting of negatively charged sulfonate-functionalized Au nanoparticles (Au-NPs) incorporated into PAn and its application as a matrix for the enhanced electrocatalysis and bioelectrocatalysis. We generate the PAn/Au-NPs composite in two configurations. One configuration includes the PAn/Au-NPs as a planar film on a gold surface, while the second configuration includes the PAn/Au-NPs composite as a microstructured system generated in the micropores of an alumina membrane. We compare the performance of the two configurations to the analogous PAn systems that lack the Au-NPs.

Experimental Section

Chemicals and Materials. Aniline, *p*-aminothiophenol, sodium borohydride, 2-mercaptoethane sulfonic acid sodium salt, β-D-glucose, ascorbic acid, poly(4-styrene-sulfonate) sodium salt (average MW ca. 70 000) (PSS), hydrogen tetrachloroaurate trihydrate, and glucose oxidase, GOx, (EC 1.1.3.4; type X−S from *Aspergillus niger*) and all other chemicals were purchased from Sigma or Aldrich and were used without further purification. Porous alumina membranes (Anodisc membrane, 25-mm size diameter, with 0.2-μm pore diameter) were purchased from Whatman. Au nanoparticles functionalized with sulfonic acid groups (Au-NPs) were prepared according to the published procedure using 2-mercaptoethane sulfonic acid as a capping material.[19] Ultrapure water from NANOpure Diamond (Barnstead) source was used throughout all the experiments.

Chemical Modification of Electrodes. Two different conductive supports were used as working electrodes: (i) A Au-coated (50-nm gold layer) glass plate (Analytical μ-Systems, Germany) was used as a working electrode with a smooth surface. (ii) A porous alumina membrane was coated with a thiolated polysiloxane film generated from 3-mercaptopropyltrimethoxysilane according to the published procedure,[20] to provide an adhesive sublayer for further Au deposition. Vacuum deposition of a Au layer was performed on one side of a silanized porous alumina membrane, and then the thickness of the conductive Au layer was increased up to 1 μm by the electrochemical deposition of Au using the Au-enhancement kit (Engold 2010, Engelhard Ltd.) under galvanostatic conditions (0.35 mA cm^{-2}) for 20 min. The generated Au-supported alumina membrane was used as a microporous working electrode. The two kinds of working electrodes (a Au smooth electrode or a Au microporous electrode) were modified by a self-assembled monolayer of *p*-aminothiophenol by reacting the Au surface with an ethanolic solution of *p*-aminothiophenol, 50 mM, for 24 h, followed by washing the electrode with ethanol. PAn/PSS or PAn/Au-NPs composite layers were generated on a conductive support (Au-coated glass slide or Au-coated alumina membrane) by the electropolymerization of aniline, 5 mM, in an electrolyte solution, pH = 1.8, composed of 0.1 M H_2SO_4 and 0.5 M Na_2SO_4, that included poly(4-styrene-sulfonate) (PSS), 1 mg mL^{-1}, or sulfonic acid-functionalized Au nanoparticles (Au-NPs), 1 mg mL^{-1}, respectively. The polymerization was performed by the application of 100 potential cycles between −0.1 and +0.9 V and potential scan rate of 100 mV s^{-1}. The resulting films were washed with the background electrolyte solution composed of 0.1 M H_2SO_4 and 0.5 M Na_2SO_4 to exclude any residual monomer from the electrode. The alumina membrane, which was used as a template for the electropolymerization process, was dissolved by reacting the electrode with 3 M NaOH for 20 min to yield the microstructured electrode surface modified with PAn/PSS or PAn/Au-NPs rod structures.

Electrochemical Measurements and Microscopy Imaging. Cyclic voltammetry measurements were performed using an electrochemical analyzer (model 6310, EG&G) connected to a personal computer with EG&G 270/250 software. The measure-

(10) (a) Kinyanjui, J. M.; Hanks, J.; Hatchett, D. W.; Smith, A.; Josowicz, M. *J. Electrochem. Soc.* **2004**, *151*, D113−D120. (b) Pauliukaite, R.; Brett, C. M. A.; Monkman, A. P. *Electrochim. Acta* **2004**, *50*, 159−167. (c) Tian, S. J.; Liu, J. Y.; Zhu, T.; Knoll, W. *Chem. Mater.* **2004**, *16*, 4103−4108.

(11) (a) Han, D. H.; Park, S. M. *J. Phys. Chem. B* **2004**, *108*, 13921−13927. (b) Zaidi, N. A.; Foreman, J. P.; Tzamalis, G.; Monkman, S. C.; Monkman, A. P. *Adv. Funct. Mater.* **2004**, *14*, 479−486. (c) Bhattacharya, A.; De, A. *Prog. Solid State Chem.* **1996**, *24*, 141−181.

(12) (a) Cao, T. B.; Wei, L. H.; Yang, S. M.; Zhang, M. F.; Huang, C. H.; Cao, W. X. *Langmuir* **2002**, *18*, 750−753. (b) Bondarenko, V. E.; Zhuravleva, T. S.; Misurkin, I. A.; Titov, S. V.; Trakhtenberg, L. I. *Chem. Phys. Rep.* **1999**, *18*, 289−306. (c) Potje-Kamloth, K.; Polk, B. J.; Josowicz, M.; Janata, J. *Adv. Mater.* **2001**, *13*, 1797−1800. (d) Huang, H. G.; Zheng, Z. X.; Luo, J.; Zhang, H. P.; Wu, L. L.; Lin, Z. H. *Synth. Met.* **2001**, *123*, 321−325.

(13) (a) Kanungo, M.; Kumar, A.; Contractor, A. Q. *Anal. Chem.* **2003**, *75*, 5673−5679. (b) Fabre, B.; Taillebois, L. *Chem. Commun.* **2003**, 2982−2983. (c) Janata, J.; Josowicz, M. *Nat. Mater.* **2003**, *2*, 19−24.

(14) Lahav, M.; Durkan, C.; Gabai, R.; Katz, E.; Willner, I.; Welland, M. E. *Angew. Chem., Int. Ed.* **2001**, *40*, 4095−4097.

(15) (a) Luo, Y. C.; Do, J. S. *Biosens. Bioelectron.* **2004**, *20*, 15−23. (b) Shi, L. X.; Xiao, Y.; Willner, I. *Electrochem. Commun.* **2004**, *6*, 1057−1060. (c) Gerard, M.; Ramanathan, K.; Chaubey, A.; Malhotra, B. D. *Electroanalysis* **1999**, *11*, 450−452.

(16) (a) Raitman, O. A.; Patolsky, F.; Katz, E.; Willner, I. *Chem. Commun.* **2002**, 1936−1937. (b) Raitman, O. A.; Katz, E.; Bückmann, A. F.; Willner, I. *J. Am. Chem. Soc.* **2002**, *124*, 6487−6496.

(17) (a) Ohsaka, T.; Ohnuki, Y.; Oyama, N.; Katagiri, K.; Kamisako, K. *J. Electroanal. Chem.* **1984**, *161*, 399−405. (b) Diaz, A. F.; Logan, J. A. *J. Electroanal. Chem.* **1980**, *111*, 111−114. (c) Cui, S. Y.; Park, S. M. *Synth. Met.* **1999**, *105*, 91−98. (d) Jannakoudakis, P. D.; Pagalos, N. *Synth. Met.* **1994**, *68*, 17−31.

(18) (a) Yue, J.; Wang, Z. H.; Cromack, K. R.; Epstein, A. J.; MacDiarmid, *J. Am. Chem. Soc.* **1991**, *113*, 2665−2671. (b) Bartlett, P. N.; Simon, E. *Phys. Chem. Chem. Phys.* **2000**, *2*, 2599−2606. (c) Bartlett, P. N.; Birkin, P. R.; Wallace, E. N. K. *J. Chem. Soc., Faraday Trans.* **1997**, *93*, 1951−1960. (c) Bartlett, P. N.; Wallace, E. N. K. *Phys. Chem. Chem. Phys.* **2001**, *3*, 1491−1496. (d) Bartlett, P. N.; Wang, J. H. *J. Chem. Soc., Faraday Trans.* **1996**, *92*, 4137−4143.

(19) Johnson, S. R.; Evans, S. D.; Brydson, R. *Langmuir* **1998**, *14*, 6639−6647.

(20) Goss, C. A.; Charych, D. H.; Majda, M. *Anal. Chem.* **1991**, *63*, 85−88.

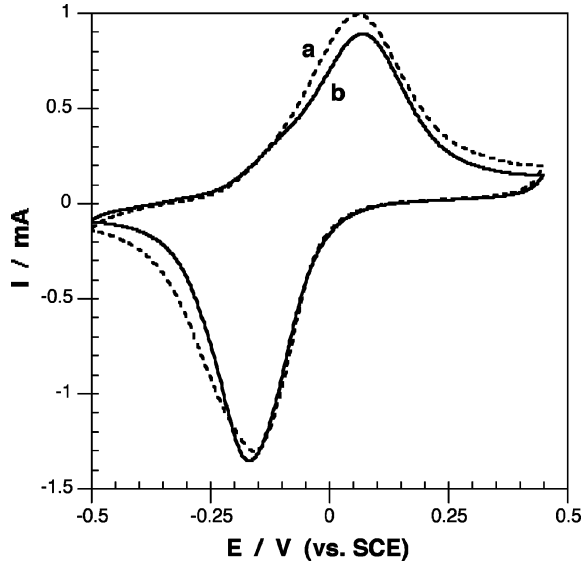

Figure 1. Cyclic voltammograms of the Au electrodes modified with the planar films composed of (a) PAn/PSS and (b) PAn/Au-NPs. The data were recorded in 0.1 M phosphate buffer, pH = 7.5. Oxygen was removed from the background solution by bubbling with Ar. Potential scan rate, 50 mV s^{-1}.

ments were carried out at ambient temperature (25 ± 2 °C) in a conventional electrochemical cell consisting of a modified Au working electrode (1.3 cm^2 geometrical area exposed to the solution) assembled at the bottom of the electrochemical cell, a glassy carbon auxiliary electrode, and a saturated calomel electrode (SCE). All potentials are reported with respect to this reference electrode. Phosphate buffer (0.1 M, pH 7.5) was used as a background electrolyte. Argon bubbling was used to remove oxygen from the solution in the electrochemical cell. The cell was placed in a grounded Faraday cage.

AFM-measurements were performed at ambient temperature conditions using a SMENA-B atomic force microscope (NT-MDT, Russia) with a SMENA-A scanner head. The cantilevers in use were NSC15/AlBS (MikroMasch, Russia) with a resonance frequency of about 280 kHz. The oscillation amplitude was between 20 and 40 nm with a damping of 50% during the measurements. Step edges were achieved by scratching the surface to remove the polymer and the gold so as to reveal the glass substrate as a reference plane. Several 60 μm by 60 μm scans of these step edges were performed, and the thickness of the polymeric layer was then calculated as the difference in height of the polymer/gold layered structure as compared to that of the gold by itself.

Results and Discussion

Aniline was electropolymerized on Au-electrodes in the presence of poly(4-styrene-sulfonate) (PSS). The electrostatic association of anilinium ions with the negatively charged PSS polymer results in a composite PAn/PSS film on the electrode. Figure 1, curve a, shows the cyclic voltammogram of the PAn/PSS film, indicating that the composite polymer reveals a quasi-reversible electrochemical process, $E^\circ = -0.05$ V, at pH = 7.5. By the coulometric assay of the PAn oxidation (or reduction) wave, the surface coverage of the PAn is estimated to be 1.9×10^{-8} mole cm^{-2} (for the redox units of PAn).

Au nanoparticles (average diameter ca. 4 nm) were functionalized with 2-mercaptoethane sulfonic acid yielding a negatively charged capping layer on the Au-NPs. Aniline was electropolymerized in the presence of the negatively charged Au-NPs (but in the absence of PSS). Figure 1, curve b, shows the cyclic voltammogram of the resulting electrode modified with the PAn/Au-NPs composite film. It is evident that the PAn/Au-NPs film exhibits a quasi-reversible electrochemical process, $E^\circ = -0.05$ V, at pH = 7.5. This is attributed to the fact that anilinium monomer units are associated to the negatively charged Au-NPs resulting in the formation of the PAn matrixes doped with the negatively charged nanoparticles. Comparison of the cyclic voltammogram of the PAn/Au-NPs composite film and the PAn/PSS composite film indicates a similar surface coverage of the electrodes, 1.9×10^{-8} mole cm^{-2}.

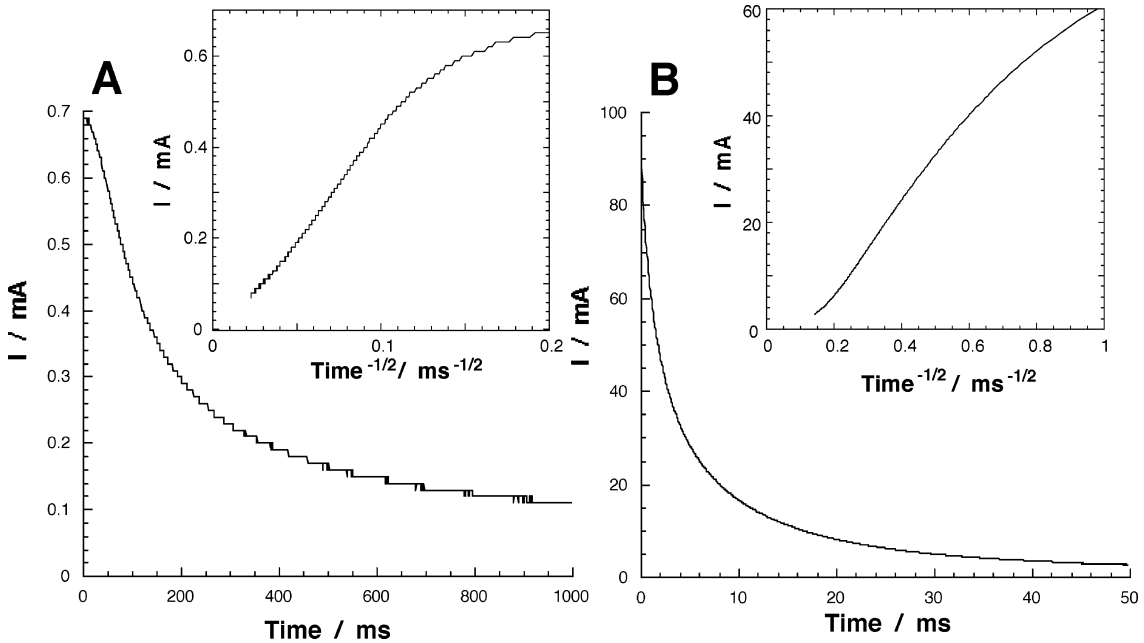

Figure 2. Chronoamperometric transients measured upon applying a potential step from −0.3 V to 0.3 V on the electrodes modified with planar films composed of (A) PAn/PSS and (B) PAn/Au-NPs. Insets: The current decays replotted as the functions of $t^{-1/2}$. The data were recorded in 0.1 M phosphate buffer, pH = 7.5. Oxygen was removed from the background solution by bubbling with Ar.

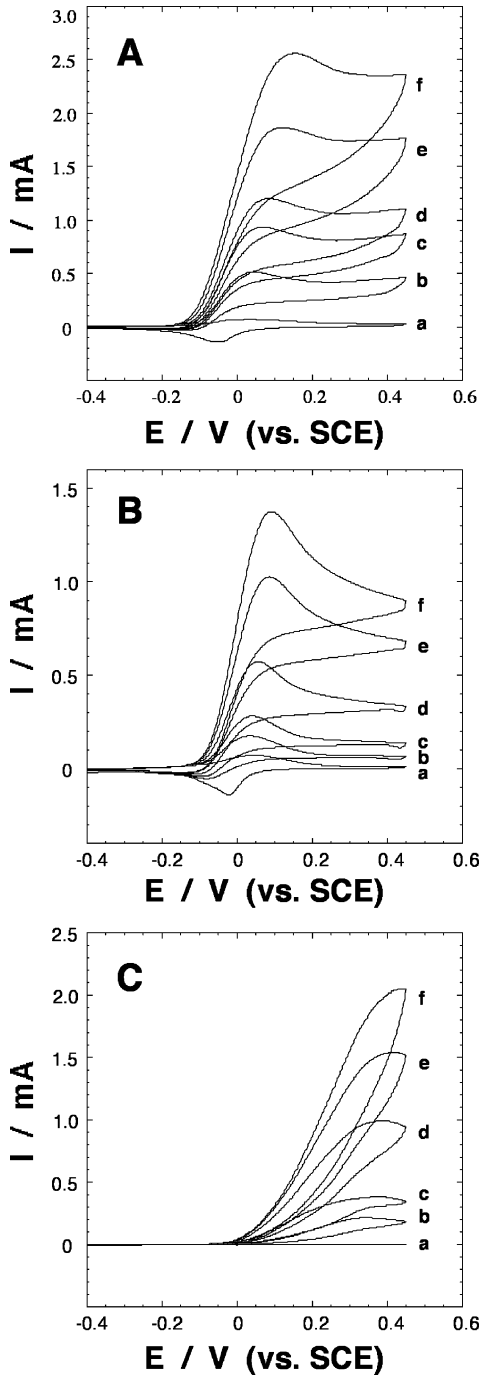

Figure 3. Electrochemical oxidation of ascorbic acid: (A) Cyclic voltammograms recorded in the presence of the planar film composed of PAn/Au-NPs and different concentrations of ascorbic acid: (a) 0 mM, (b) 5 mM, (c) 10 mM, (d) 20 mM, (e) 30 mM, and (f) 40 mM. (B) Cyclic voltammograms recorded in the presence of the planar film composed of PAn/PSS and different concentrations of ascorbic acid: (a) 0 mM, (b) 5 mM, (c) 10 mM, (d) 20 mM, (e) 30 mM, and (f) 40 mM. (C) Cyclic voltammograms recorded in the presence of the bare Au electrode and different concentrations of ascorbic acid: (a) 0 mM, (b) 5 mM, (c) 10 mM, (d) 20 mM, (e) 30 mM, and (f) 40 mM. The data were recorded in 0.1 M phosphate buffer, pH = 7.5. Oxygen was removed from the background solution by bubbling with Ar. Potential scan rate, 5 mV s^{-1}.

To determine the thickness of the polymeric layers, the samples were scratched, and the resulting profiles were imaged with an AFM. Both samples revealed approximately the same thickness of 90 nm ± 5 nm and 95 nm ± 10 nm for the PAn/PSS composite film and for the PAn/Au-NPs composite film, respectively. Taking into account the polymer thickness, the concentrations of the redox polymer units in the films can be calculated to be ca. 2.1×10^{-8} mole cm^{-3} and ca. 2.0×10^{-8} mole cm^{-3} for the PAn/PSS system and the PAn/Au-NPs system, respectively. To find the amount of Au associated with the composite film, the polymerization procedure was performed on a graphite electrode, the PAn/Au-NPs composite film was dissolved in HCl/HNO_3 mixture (3:1 volume ratio), and the solution was analyzed by inductively coupled plasma-optical emission spectroscopy (ICP−OES). The amount of Au in the similar composite film on the Au electrode support (normalized according to the charge associated with the redox polymer films on the graphite and on the Au support) was ca. 63 μg per electrode. Taking into account the gold density (19.3 g cm^{-3}), the electrode area (0.3 cm^3), and the thickness of the composite film (95 nm), one can calculate that the Au-NPs occupy ca. 25% of the volume of the PAn/Au-NPs composite film.

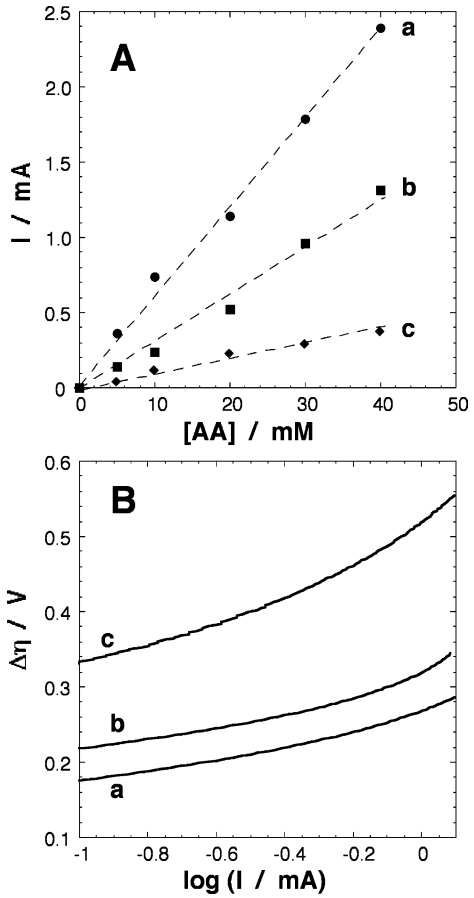

Figure 4. (A) Calibration plots corresponding to the electrochemical oxidation of ascorbic acid derived from the cyclic voltammograms at E = 0.1 V: (a) for the PAn/Au-NPs system, (b) for the PAn/PSS system, (c) for the bare Au electrode. (B) Tafel plots corresponding to the electrochemical oxidation of ascorbic acid: (a) for the PAn/Au-NPs system, (b) for the PAn/PSS system, (c) for the bare Au electrode.

The understanding of the charge transport through conductive polymers and particularly polyaniline films has attracted substantial research efforts.[21] Kinetics of the electrochemical processes occurring in redox polymers can be characterized by chronopotentiometry.[22] In general, the current transient

(21) (a) Otero, T. F.; Boyano, I. *J. Phys. Chem. B* **2003**, *107*, 4269−4276. (b) Vorotyntsev, M. A.; Levi, M. D.; Aurbach, D. *J. Electroanal. Chem.* **2004**, *572*, 299−3077.

Scheme 1. Bioelectrocatalytic Oxidation of Glucose by Solubilized GOx and Mediated by the Planar Films Composed of (A) PAn/PSS and (B) PAn/Au-NPs

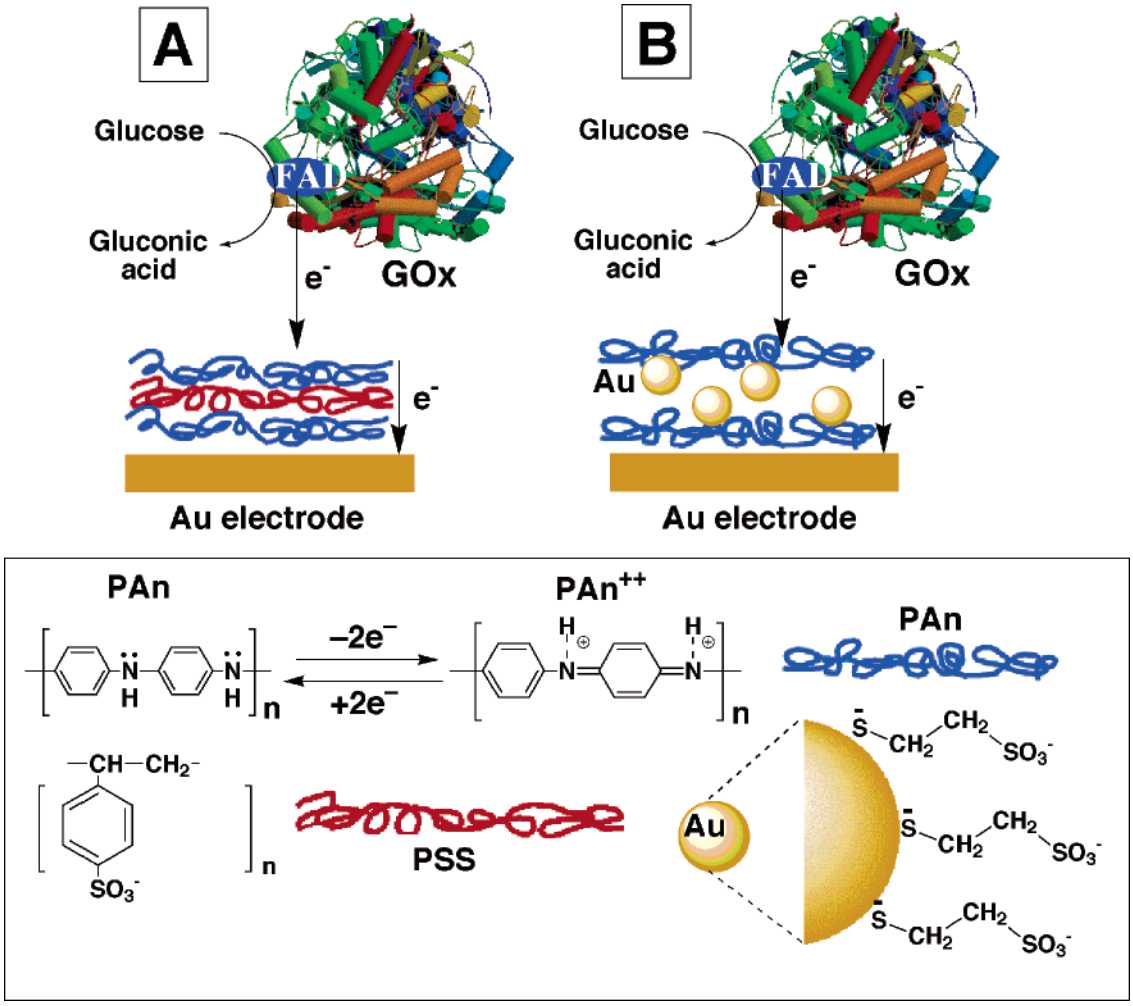

generated upon application of a potential step on redox polymer-modified electrodes obeys the Cottrell equation (eq 1),[23] in which I (A) is the current transient that decays in the course of time t (s), n is the number of electrons per unit of the redox polymer ($n = 2$ for polyaniline), F is the Faraday constant (C equiv^{-1}), A is the electrode area (cm^2), D is the diffusion coefficient for the charge propagation in the polymer film (cm^2 s^{-1}), and C is the concentration of the redox units in the polymer film (mole cm^{-3}).

$$I = nFAC\sqrt{\frac{D}{\pi t}} \qquad (1)$$

Figure 2A shows the chronoamperometric transient of the PAn/PSS film upon the application of an oxidative potential step from −0.3 V to 0.3 V. The anodic current transient decays on a time scale of ca. 900 ms. Figure 2B shows the chronoamperometric transient of the PAn/Au-NPs film. The anodic current transient in this system decays on a time scale corresponding to ca. 50 ms, indicating a substantially faster electron-transfer process through the PAn/Au-NPs composite film as compared to the PAn/PSS composite film. Upon applying the Cottrell equation to the experimental current transients, one could predict a linear relation between the current evolution as $t^{-1/2}$. To analyze the rate of the charge propagation in the composite redox polymers following the Cottrell equation, the experimental current transients were replotted as functions of $t^{-1/2}$, Figure 2A and B insets. The calculated transient curves reveal reasonable linearity for the major parts of the plots, but some deviations from the theoretically expected linearity are observed at high current values. These deviations could originate from the nonhomogeneity of the composite films (in their thickness and composition). Applying the Cottrell equation to the linear parts of the current versus $t^{-1/2}$, we calculated the ratio of the effective values of the charge propagation diffusion coefficients for the PAn/Au-NPs and PAn/PSS composite films to be ca. 250. The enhanced electron transfer in the PAn/Au-NPs system is attributed to the charge hopping through the metallic conductive Au nanoparticles that mediate the effective charge migration through the polymer.

To follow the effect of the enhanced charge transport of the PAn/Au-NPs composite on electrochemical processes at the modified electrode, we examined the electrochemical oxidation of ascorbic acid (AA) by the PAn/Au-NPs-

(22) Hillman, A. R. In *Electrochemical Science and Technology of Polymers*; Linford, R. G., Ed.; Elsevier: New York, 1987; Vol. 1, pp 103−239.
(23) (a) Cottrell, F. G. *Z. Phys. Chem.* **1902**, *42*, 385. (b) Bard, A. J.; Faulkner, L. R. *Electrochemical Methods: Fundamentals and Applications*; Wiley: New York, 1980; p 143.

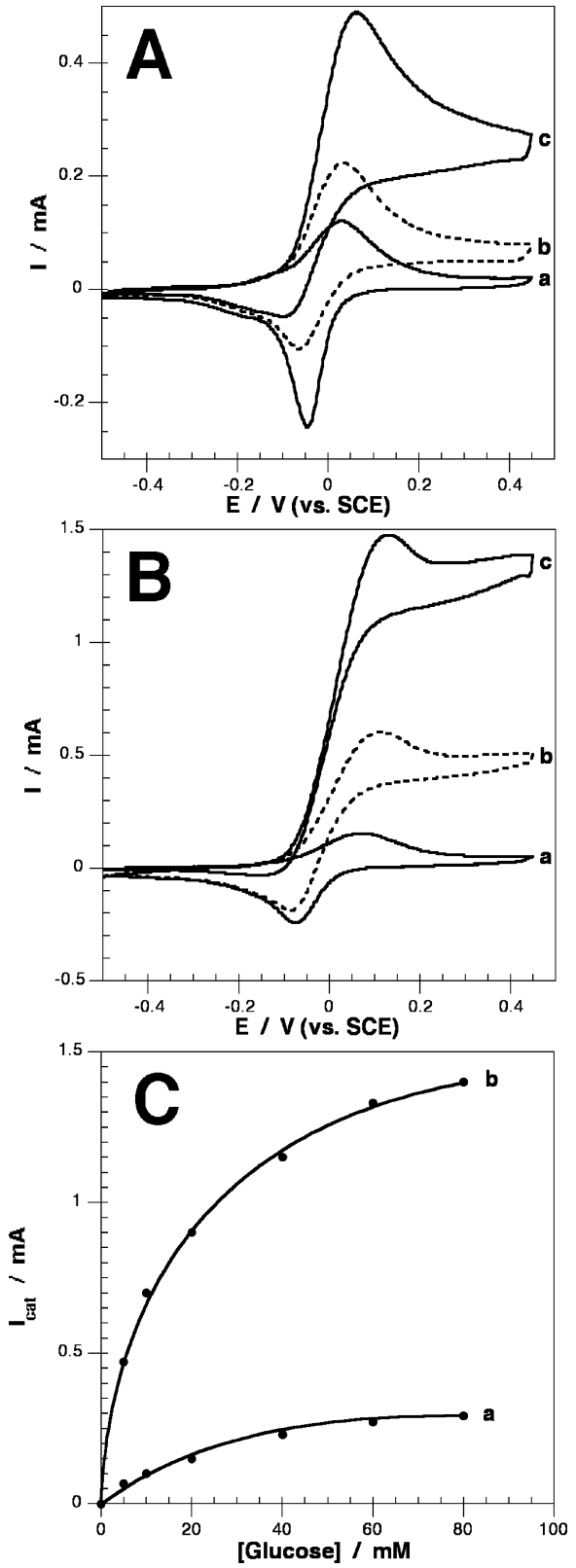

Figure 5. Bioelectrocatalytic oxidation of glucose by solubilized GOx, 1 mg mL^{-1}, and mediated by the composite redox-active planar films: (A) Cyclic voltammograms recorded in the presence of the planar film composed of PAn/PSS and different concentrations of glucose: (a) 0 mM, (b) 5 mM, and (c) 80 mM. (B) Cyclic voltammograms recorded in the presence of the planar film composed of PAn/Au-NPs and different concentrations of glucose: (a) 0 mM, (b) 5 mM, and (c) 80 mM. (C) Calibration plots derived from the cyclic voltammograms at $E = 0.4$ V: (a) for the PAn/PSS system, (b) for the PAn/Au-NPs system. The data were recorded in 0.1 M phosphate buffer, pH = 7.5. Oxygen was removed from the background solution by bubbling with Ar. Potential scan rate, 5 mV s^{-1}.

functionalized electrode and compared the results to the electrocatalytic oxidation of AA by the PAn/PSS-modified electrode, Figure 3A and B. The electrocatalyzed oxidation of AA by the PAn/Au-NPs is ca. 2-fold more efficient than in the PAn/PSS system (the two electrodes include the same content of PAn, ca. 1.9×10^{-8} mole cm^{-2}). For comparison, we studied also the oxidation of AA by the bare Au electrode, Figure 3C. The anodic current is observed at more positive potentials than with the PAn-modified electrodes, implying that the polymer matrixes act as catalysts for the oxidation of AA. Figure 4A shows the anodic current (at $E = 0.1$ V) developed by the two PAn-modified electrodes and the bare Au electrode. Figure 4B shows the Tafel plots corresponding to the oxidation of AA by the three electrodes (taking into account the thermodynamic potential of AA, $E° = 58$ mV vs NHE).[24] The overpotential reqired for the oxidation of AA is controlled by the modifier associated with the electrode, and the lowest overpotential is observed with the PAn/Au-NPs modified film. This result is consistent with the enhanced charge transport through the PAn/Au-NPs system.

The electrical contacting of redox-proteins with electrode surfaces attracts substantial research efforts[25] directed to the development of electrochemical biosensors[26] and biofuel cell devices.[27] Conductive polymers[28] and specifically polyaniline[29] proved to be redox-active matrixes for the electron-transfer-mediated electrical contacting of redox enzymes, such as glucose oxidase (GOx). We have applied the PAn/PSS film-modified electrode and the PAn/Au-NPs-modified electrode as active interfaces for the bioelectrocatalyzed oxidation of glucose in the presence of GOx, Scheme 1. Figure 5A shows the cyclic voltammograms obtained in the PAn/PSS system in the absence of glucose, curve a, and with

(24) *CRC Handbook of Biochemistry and Molecular Biology*, 3rd ed.; Fasman, G. D., Ed.; CRC Press: Cleveland, OH, 1976; Vol. 1, pp 122−130.

(25) (a) Katz, E.; Shipway, A. N.; Willner, I. In *Encyclopedia of Electrochemistry*; Wilson, G. S., Bard, A. J., Stratmann, M., Eds.; Wiley-VCH: Weinheim, Germany, 2002; Vol. 9, Chapter 17, pp 559−626. (b) Willner, I.; Katz, E. *Angew. Chem., Int. Ed.* **2000**, *39*, 1180−1218. (c) Heller, A. *Acc. Chem. Res.* **1990**, *23*, 128−134. (d) Armstrong, F. A.; Wilson, G. S. *Electrochim. Acta* **2000**, *45*, 2623−2645.

(26) (a) Turner, A. P. F. *Science* **2000**, *290*, 1315−1317. (b) Xiao, Y.; Patolsky, F.; Katz, E.; Hainfeld, J. F.; Willner, I. *Science* **2003**, *299*, 1877−1881. (c) Katz, E.; Sheeney-Ichia, L.; Willner, I. *Angew. Chem., Int. Ed.* **2004**, *43*, 3292−3300.

(27) (a) Katz, E.; Shipway, A. N.; Willner, I. In *Handbook of Fuel Cells*—Fundamentals, Technology, Applications; Vielstich, W., Gasteiger, H., Lamm, A., Eds.; Wiley: New York, 2003; Vol. 1, Part 4, Chapter 21, pp 355−381. (b) Katz, E.; Willner, I.; Kotlyar, A. B. *J. Electroanal. Chem.* **1999**, *479*, 64−68. (c) Katz, E.; Willner, I. *J. Am. Chem. Soc.* **2003**, *125*, 6803−6813. (d) Mano, N.; Mao, F.; Heller, A. *J. Am. Chem. Soc.* **2003**, *125*, 6588−6594. (e) Heller, A. *Phys. Chem. Chem. Phys.* **2004**, *6*, 209−216.

(28) (a) Curulli, A.; Valentini, F.; Orlanduci, S.; Terranova, M. L.; Palleschi, G. *Biosens. Bioelectron.* **2004**, *20*, 1223−1232. (b) Sharma, S. K.; Singhal, R.; Malhotra, B. D.; Sehgal, N.; Kumar, A. *Biosens. Bioelectron.* **2004**, *20*, 651−657. (c) Yang, M. H.; Yang, Y. H.; Yang, Y.; Shen, G. L.; Yu, R. Q. *Anal. Biochem.* **2004**, *334*, 127−134. (d) Tatsuma, T.; Sato, T. *J. Electroanal. Chem.* **2004**, *572*, 15−19.

(29) (a) Langer, J. J.; Filipiak, M.; Kecinska, J.; Jasnowska, J.; Wlodarczak, J.; Buladowski, B. *Surf. Sci.* **2004**, *573*, 140−145. (b) Pan, X. H.; Kan, J. Q.; Yuan, L. M. *Sens. Actuators, B* **2004**, *102*, 325−330. (c) Mathebe, N. G. R.; Morrin, A.; Iwuoha, E. I. *Talanta* **2004**, *64*, 115−120. (d) Borole, D. D.; Kapadi, U. R.; Mahulikar, P. P.; Hundiwale, D. G. *Polym. Adv. Technol.* **2004**, *15*, 306−312. (e) Kan, J. Q.; Pan, X. H.; Chen, C. *Biosens. Bioelectron.* **2004**, *19*, 1635−1640.

Scheme 2. Bioelectrocatalytic Oxidation of Glucose by Solubilized GOx and Mediated by the Microstructured Assemblies Composed of (A) PAn/PSS and (B) PAn/Au-NPs

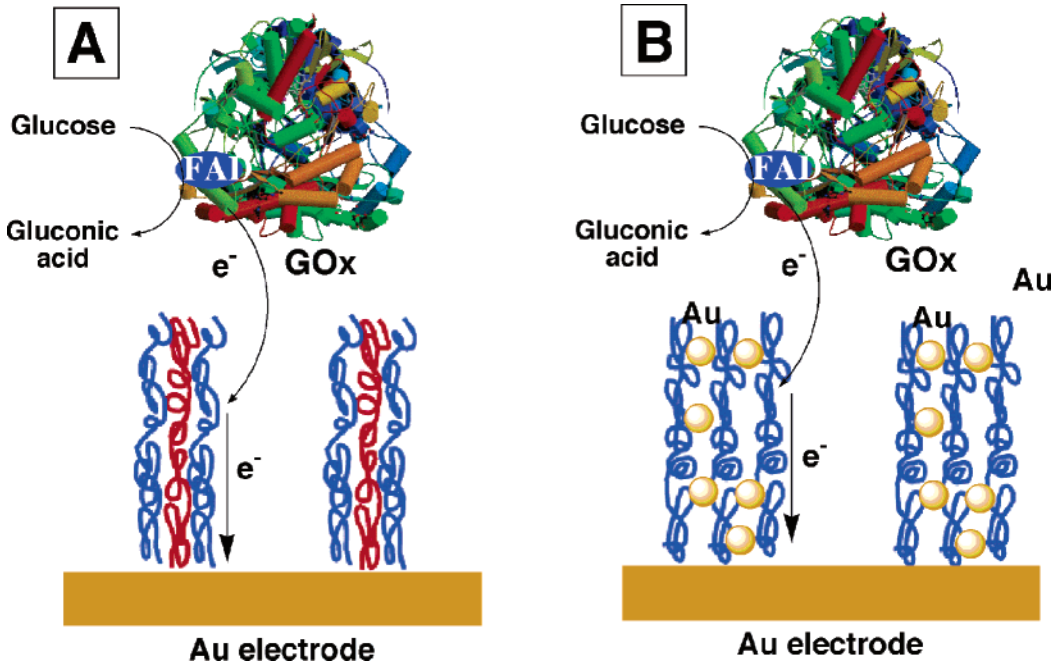

variable concentrations of glucose, curves b and c. The observed electrocatalytic anodic currents imply that the PAn/PSS film activates the bioelectrocatalytic oxidation of glucose by the mediated electron transfer from the enzyme redox center to the electrode, Scheme 1A. As the concentration of glucose increases, the electrocatalytic anodic current is higher, and it levels off at a glucose concentration corresponding to ca. 80 mM. At this glucose concentration, the active site of the biocatalyst is saturated and the bioelectrocatalytic performance of the system proceeds at its highest turnover rate. Figure 5C, curve a, shows the derived calibration curve. Figure 5B shows the cyclic voltammograms observed upon the bioelectrocatalyzed oxidation of glucose by GOx mediated by the PAn/Au-NPs-modified electrode in the absence, curve a, and the presence of different concentrations of glucose, curves b and c, respectively. Figure 5C, curve b, shows the derived calibration curve corresponding to the anodic currents (E = 0.4 V) generated at the different concentrations of glucose. The bioelectrocatalytic anodic currents increase as the concentration of glucose in the system is elevated and level off at a glucose concentration corresponding to 80 mM. The results imply, however, that the bioelectrocatalytic oxidation of glucose mediated by the PAn/Au-NPs system is significantly improved when compared to the PAn/PSS system. The content of the redox-active PAn polymer associated with the two electrodes is identical. The electrocatalytic anodic currents are, however, ca. 4.6-fold higher in the PAn/Au-NPs system as compared to the PAn/PSS assembly. For example, at a glucose concentration of 80 mM, the PAn/Au-NPs system generates an anodic current of 1.4 mA, whereas the PAn/PSS system yields a current of 0.3 mA. The improved bioelectrocatalytic oxidation of glucose by the PAn/Au-NPs system is attributed to the enhanced charge transport through the Au-NPs composite system that facilitates the electrical contacting of the redox enzyme with the electrode. The accelerated oxidation of the redox center of the enzyme by the redox polymer, as a result of the effective transport of the electrons to the electrode in the PAn/Au-NPs matrix, leads to the efficient bioelectrocatalytic oxidation of glucose.

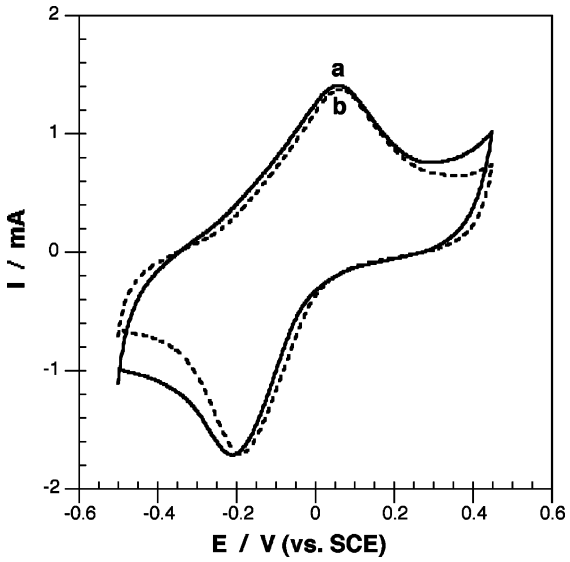

Figure 6. Cyclic voltammograms of the Au electrodes modified with the microstructured rod assemblies composed of (a) PAn/PSS and (b) PAn/Au-NPs. The data were recorded in 0.1 M phosphate buffer, pH = 7.5. Oxygen was removed from the background solution by bubbling with Ar. Potential scan rate, 50 mV s^{-1}.

The system has been further developed by the microstructuring of the electrodes with microrods of the PAn/PSS or PAn/Au-NPs matrixes and by examining the effects of the resulting microstructures on the bioelectrocatalytic functions of the matrixes. The electrochemical assembly of microrod structures on surfaces has been a subject of extensive research in the past few years.[30] The construction of the microrods is based on the deposition of a metal on one side of a porous membrane and the electrochemical reduction or oxidation

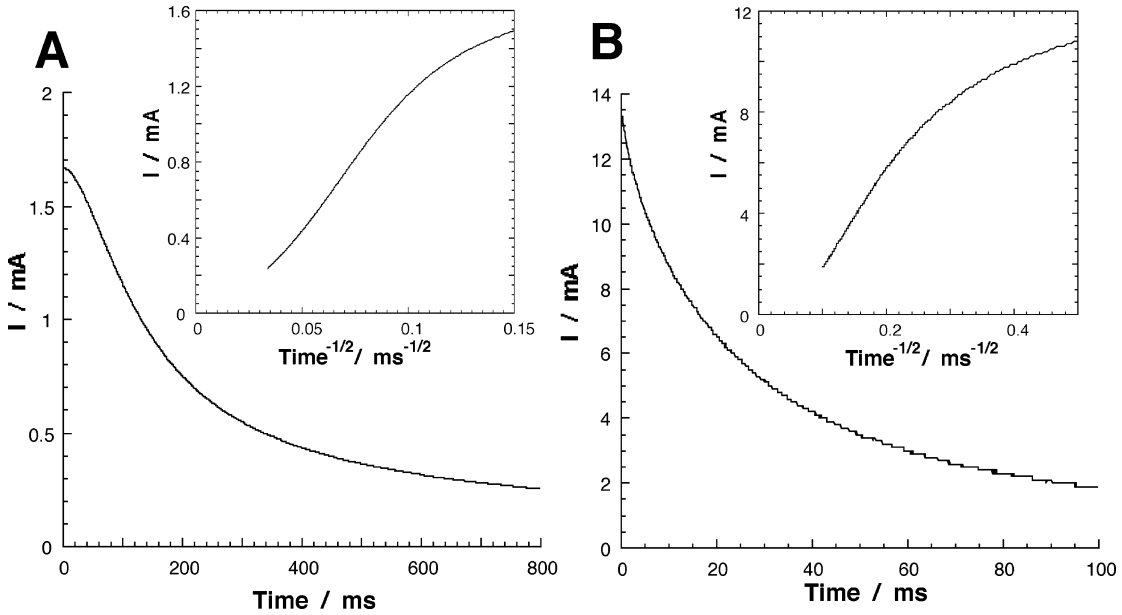

Figure 7. Chronoamperometric transients measured upon applying a potential step from −0.3 to 0.3 V on microstructured rod assemblies composed of (A) PAn/PSS and (B) PAn/Au-NPs. Insets: The current decays are replotted as the functions of $t^{-1/2}$. The data were recorded in 0.1 M phosphate buffer, pH = 7.5. Oxygen was removed from the background solution by bubbling with Ar.

of redox-active solubilized compounds in the membrane pores. The subsequent dissolution of the membrane leads then to the formation of microstructures generated in the membrane template pores on the electrode support. Different microrod structures, including metals,[31] polymers,[32] and composite materials,[31a,33] were generated on electrodes by this method.

The PAn/PSS or the PAn/Au-NPs systems were constructed in the pores of an alumina membrane coated with a Au film on one side, and the composite-polymer microrods were generated on the electrode by the dissolution of the membrane, Scheme 2. Figure 6 shows the cyclic voltammograms of PAn/PSS and PAn/Au-NP systems that were generated in the membrane pores by electropolymerization of aniline in the presence of PSS, curve a, and in the presence of Au-NPs, curve b, respectively. The amount of the electroactive polymer in the two systems is comparable, 1.9 $\times$ 10^{-8} mole cm^{-2}, as derived from the respective cyclic voltammograms. Also, the amount of the electrochemically active polymer generated in the pores is comparable to that described in the previous PAn/PSS and PAn/Au-NPs systems generated in the form of the smooth films. The length of the PAn/Au-NPs microrods is in the range of 350−850 nm according to the SEM imaging (vide infra for the detailed discussion).

Figure 7A and B shows the chronoamperometric transients observed upon the application of an oxidation step on the microstructured polymer assemblies. As described earlier, the current decays were replotted as functions of $t^{-1/2}$, Figure 7A and B insets, and from the linear parts of the plots, we calculated the ratio of the effective values of the charge propagation diffusion coefficients for the PAn/Au-NPs and PAn/PSS composite microstructured rods to be ca. 7. The enhanced electron transfer in the PAn/Au-NPs system is attributed to the charge hopping through the metallic conductive Au nanoparticles that mediate the effective charge migration through the polymer.

Figure 8A shows the cyclic voltammograms of the PAn/PSS microrod structures generated in the membrane in the presence of the solubilized GOx in the absence, curve a, and the presence, curve b, of different glucose concentrations, respectively. Figure 8B shows the cyclic voltammograms corresponding to the PAn/Au-NPs system in the presence of the solubilized GOx in the absence, curve a, of glucose and in the presence of different concentrations of glucose, curves b and c, respectively. Figure 8C, curve a and curve b, shows the derived calibration curves for the PAn/PSS and PAn/Au-NPs systems assembled in the microrod assemblies, respectively. From these results and upon their comparison to the planar polymer film configurations, the following conclusion can be made: (i) Although the content of redox-active polymers associated with the electrodes is comparable, in the planar composite films and the microstructured rod configurations, the bioelectrocatalytic currents observed in the presence of the microrod structures are substantially higher than in the planar film assemblies. For the PAn/PSS system, the anodic current generated by the microrod system is ca. 3-fold higher than in the planar film configuration, albeit the content of the electroactive polymer associated with

(30) (a) Hsu, C. L.; Yang, S. S.; Tseng, Y. K.; Chen, I. C.; Lin, Y. R.; Chang, S. J.; Wu, S. T. *J. Phys. Chem. B* **2004**, *108*, 18799−18803. (b) Li, Z. Q.; Ding, Y.; Xiong, Y. J.; Yang, Q.; Xie, Y. *Chem. Eur. J.* **2004**, *10*, 5823−5828. (c) Park, J. H.; Park, J. G. *Appl. Phys. A* **2005**, *80*, 43−46. (d) Ho, G. W.; Wong, A. S. W.; Wee, A. T. S.; Welland, M. E. *Nano Lett.* **2004**, *4*, 2023−2026.

(31) (a) Martin, C. R. *Science* **1994**, *266*, 1961−1966. Nishizawa, M.; Menon, V. P.; Martin, C. R. *Science* **1995**, *268*, 700−702. (c) Kohli, P.; Wharton, J. E.; Braide, O.; Martin, C. R. *J. Nanosci. Nanotechnol.* **2004**, 4, 605−610. (d) Wirtz, M.; Martin, C. R. *Adv. Mater.* **2003**, *15*, 455−458. (e) Keating, C. D.; Natan, M. J. *Adv. Mater.* **2003**, *15*, 451−454.

(32) (a) Yamada, K.; Gasparac, R.; Martin, C. R. *J. Electrochem. Soc.* **2004**, *151*, E14−E19. (b) Sapp, S. A.; Mitchell, D. T.; Martin, C. R. *Chem. Mater.* **1999**, *11*, 1183−1187.

(33) Routkevitch, D.; Bigioni, T.; Moskovits, M.; Xu, J. M. *J. Phys. Chem.* **1996**, *100*, 14037−14047.

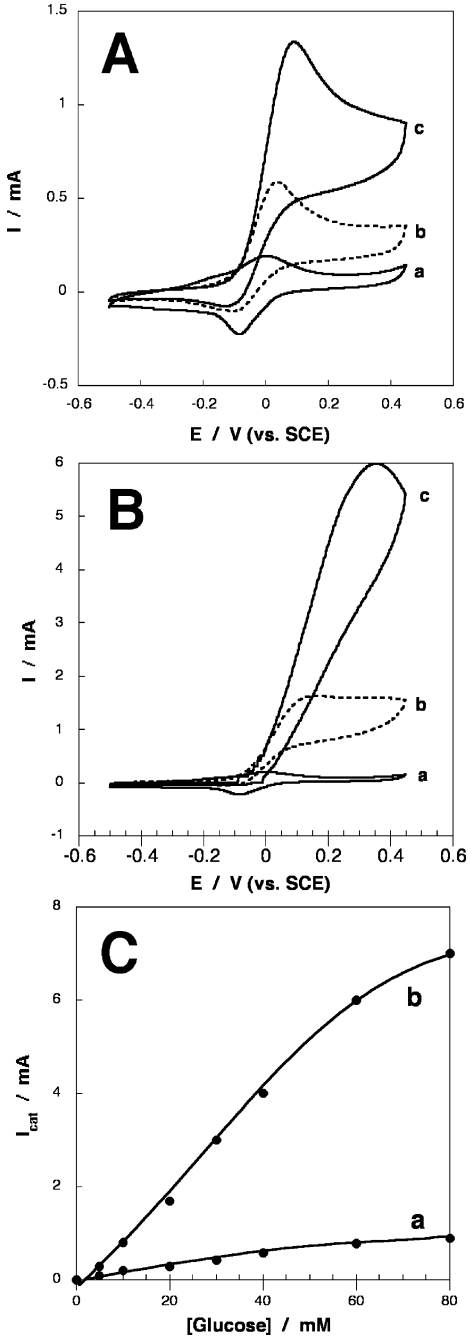

Figure 8. Bioelectrocatalytic oxidation of glucose by solubilized GOx, 1 mg mL^{-1}, and mediated by the microstructured redox-active rod assemblies: (A) Cyclic voltammograms recorded in the presence of the microstructured assemblies composed of PAn/PSS and different concentrations of glucose: (a) 0 mM, (b) 10 mM, and (c) 60 mM. (B) Cyclic voltammograms recorded in the presence of the microstructured assemblies composed of PAn/Au-NPs and different concentrations of glucose: (a) 0 mM, (b) 10 mM, and (c) 60 mM. (C) Calibration plots derived from the cyclic voltammograms at $E = 0.4$ V: (a) for the PAn/PSS system, (b) for the PAn/Au-NPs system. The data were recorded in 0.1 M phosphate buffer, pH = 7.5. Oxygen was removed from the background solution by bubbling with Ar. Potential scan rate, 5 mV s^{-1}.

the electrodes in the two systems is almost identical. Similarly, the anodic bioelectrocatalytic current generated by the PAn/Au-NPs system is ca. 5-fold higher in the presence of the microrod structure of the polymer, as compared to PAn/Au-NPs planar film assembly. (ii) The bioelectrocatalytic oxidation of glucose by the microrod PAn/Au-NPs structure is ca. 10-fold enhanced as compared to

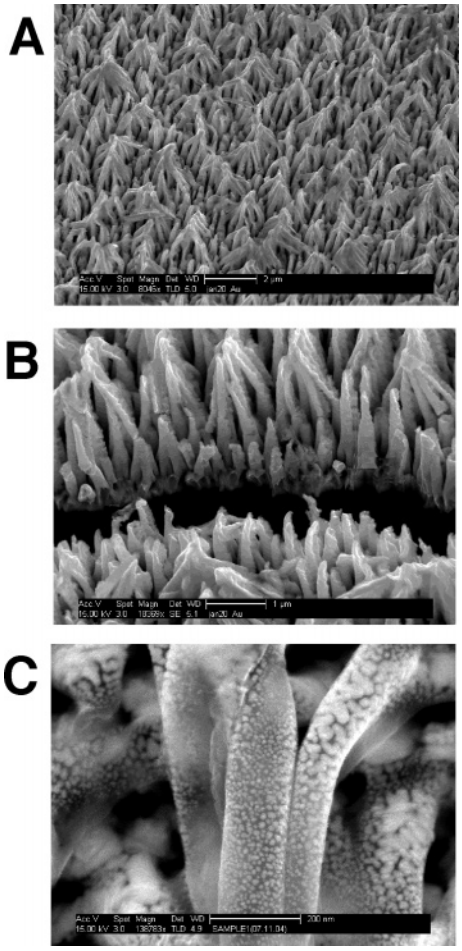

Figure 9. Scanning electron microscopy (SEM) images of (A) The PAn/Au-NPs microstructured rod assembly after dissolution of the membrane. (B) Cross section of the PAn/Au-NPs rod assembly. (C) Single-branched rod generated in the pore.

the bioelectrocatalytic oxidation of glucose by the PAn/PSS microrods. The enhanced bioelectrocatalytic oxidation of glucose by the microrod systems as compared to the respective planar film structures is attributed to the higher surface area of the microstructured polymers. The higher surface area of the electroactive polymers exposed to the electrolyte solution facilitates the electrical contacting of the solubilized enzyme GOx, resulting in the improved bioelectrocatalysis and higher bioelectrocatalytic anodic currents. The enhanced bioelectrocatalyzed transformations in the presence of the PAn/Au-NPs systems (in the planar film or rod configurations), as compared to the analogous systems lacking the Au-NPs, is attributed to the improved charge-transport properties of the Au-NP-modified polymers, as evident from the chronoamperometric experiments. The Au nanoparticles embedded into the redox polymer facilitate the electrical contacting of the enzyme redox sites with the electrode, thus accelerating the bioelectrocatalyzed oxidation of glucose. The calibration curve for the bioelectrocatalyzed oxidation of glucose by the plane PAn/Au-NPs-functionalized electrode leads to a saturation value for the glucose concentrations greater than 20 mM, while in the microrod structure of the PAn/Au-NPs system the calibration curve is linear up to ca. 60 mM of glucose and tends to a saturation value at substantially higher concentration. This result is consistent with the fact that the higher surface area of the

microrod assembly leads to the enhanced regeneration of the biocatalyst in its oxidized state, and thus saturation of the enzyme will be reached at higher glucose concentrations.

The PAn/Au-NPs microstructured rods generated in the alumina membrane were analyzed by scanning electron microscopy (SEM), Figure 9. After the dissolution of the alumina membrane, the coverage of the surface with the PAn/Au-NPs microrods is observed. The microrods reveal steric flexibility and touch one another, Figure 9A. Upon scratching of the surface and imaging the assembly cross section, Figure 9B, the height distribution of the microrods is 350−850 nm. This value is consistent with the thickness of the porous alumina membrane, the surface coverage of the pores, and the total amount of PAn generated in the pores and quantitatively analyzed by cyclic voltammetry. The structure of an individual "rod" generated in the membrane pore is depicted in Figure 9C. The rod consists of a branch of subrods that originate from the polymer "stem" associated with the bare gold electrode. This might suggest that polymerization is initiated on different surface sites of the bare gold surface, resulting in the independent growth of the polymer branches. Furthermore, it can be seen that after dissolution of the membrane the branched polymer rod occupies a volume that is larger than the original pore dimensions (200 nm diameter). This could originate from the electrostatic repulsion between the positively charged branched arms and from the swelling of the polymer as a result of the dissolution of the membrane.

In conclusion, the present study has demonstrated superior charge-transport properties through a composite PAn/Au-NPs material as compared to a PAn/PSS system. The enhanced charge-transport properties in the PAn/Au-NPs composite system were demonstrated in a planar film configuration as well as in a microstructured rods assembly. The latter assembly of the PAn/Au-NPs microrods reveals further advantages originating from the high surface area of the conductive polymer array of microrods exposed to the electrolyte solution. The study has also demonstrated the coupling of the new materials to redox proteins and the enhanced electrical contacting of the enzyme glucose oxidase by means of the PAn/Au-NPs systems in the film or microrod configurations.

Acknowledgment. This research was supported by The Israel Science Foundation (grant #847/04).

CM050193V